

## Combined description of $\bar{N}N$ scattering and annihilation with a hadronic model

V. Mull<sup>1</sup> and K. Holinde<sup>1,2</sup>

<sup>1</sup>*Institut für Kernphysik (Theorie), Forschungszentrum Jülich GmbH, D-52425 Jülich, Germany*

<sup>2</sup>*Departamento de Física Teórica, Facultad de Ciencias Físicas, Universidad de Valencia, Burjassot (Valencia), Spain*

(Received 4 November 1994)

A model for the nucleon-antinucleon interaction is presented which is based on meson-baryon dynamics. The elastic part is the  $G$ -parity transform of the Bonn  $NN$  potential. Annihilation into two mesons is described in terms of microscopic baryon-exchange processes including all possible combinations of  $\pi, \eta, \rho, \omega, a_0, f_0, a_1, f_1, a_2, f_2, K, K^*$ . The remaining annihilation part is taken into account by a phenomenological energy- and state-independent optical potential of Gaussian form. The model enables a simultaneous description of nucleon-antinucleon scattering and annihilation phenomena with fair quality.

PACS number(s): 13.75.Cs, 14.20.Dh, 21.30.+y

### I. INTRODUCTION

Quantum chromodynamics (QCD) is the theory of strong interactions with quarks and gluons representing the fundamental degrees of freedom. Nevertheless, in the low-energy regime, an effective theory in terms of collective, hadronic degrees of freedom is probably the most efficient way to quantitatively describe most strong interaction phenomena. In principle, the formulation and treatment of QCD can be done in terms of either the fundamental or the collective variables. It is a matter of convenience which set to choose under specific circumstances. Of course, because of the enormous complexity of the theory, this issue is of decisive importance when it comes to actual calculations.

From this viewpoint, quark effects in low- and medium-energy physics have to be defined as phenomena which cannot be understood in terms of only a few hadronic variables but, on the other hand, have a simple quark-gluon interpretation. In order to unambiguously prove (or disprove) the existence of such signals in nuclear physics it is essential to treat as many hadronic reactions as possible from a conventional viewpoint, in terms of baryons and mesons. Only in this way will one be able to reliably explore the limits of the conventional framework and possibly establish discrepancies with the empirical situation which might then be identified with explicit quark-gluon effects.

Reactions involving antinucleons (for a review see, e.g., the papers by Amsler and Myhrer [1] and Dover *et al.* [2]) have always been considered to be the ideal place for finding quark effects since annihilation phenomena from the nucleon-antinucleon ( $\bar{N}N$ ) system are supposedly governed by short-distance physics.

There is general consensus that for large and medium distances ( $r > 1$  fm) the elastic  $\bar{N}N$  interaction is well described in terms of meson exchanges and can be reliably obtained from a  $G$ -parity transform of suitable  $NN$  models. On the other hand, for short distances, there is at present no reliable theory in this sector. Therefore, the common attitude (taken, e.g., by the Nijmegen [3] and

Paris [4] groups) is to content oneself with a phenomenological parametrization of this region. Both groups have about 30 parameters at their disposal and obtain impressive fits to the wealth of existing experimental data. The hope (expressed by the Paris group) is that the short-range  $\bar{N}N$  interaction so determined provides “valuable hints in the elaboration of a deeper theoretical model” [4].

One should realize of course that such a method can only provide constraints but no unique answer. First of all, there are still differences and ambiguities in the medium-range part of the  $G$ -parity-transformed potentials: Different  $NN$  potentials can be used to start from; there are uncertainties due to missing contributions (like, e.g., correlated  $\rho\pi$  exchange [5]) and vertex form factor effects, which all reach out up to 1.5 fm or so. All these topics should affect the result for the short-range piece. Moreover, the usual parametrization in Ref. [4] assumes a very restricted nonlocality structure. Consequently we believe that a reliable test of a microscopic model can only be made by confronting it with the experimental data directly.

The development of a dynamical model for the short-range region is undoubtedly a formidable challenge, but it has to be met if we want to learn something about the short-range dynamics and not give up from the beginning. In order to prove the relevance of quark effects, it is not sufficient to construct a quark-gluon model which reasonably well describes the empirical situation. The (possible) breakdown of the conventional hadronic picture, which is well established in the outer-range part, has to be shown by pointing out specific discrepancies between model predictions and empirical data. This is precisely the motivation for our studies of the  $\bar{N}N$  sector, within the conventional framework, which we began almost 10 years ago.

Clearly, the goals of such a program are completely different from those typically advocated by the Nijmegen and Paris groups [3,4]. For us the main aim is to test, without any bias, a conventional dynamical model for the short-range part. Thus, it would even be counterproduc-

tive to introduce sufficient parameters in order to obtain a quantitative fit to  $\bar{N}N$  data since to do so would inhibit any conclusions about the physical relevance of the model. Also, it is obviously essential to treat the short-range piece of both the elastic and annihilation interaction in a consistent scheme.

Throughout, we use the  $G$ -parity-transformed (full) Bonn  $NN$  potential [6] as the elastic  $\bar{N}N$  interaction. This interaction has the advantage (essential for our purpose) that it is prescribed everywhere, i.e., also for (arbitrarily) short distances. Thus we are not forced to introduce any *ad hoc* parameters and so lose the predictiveness of our model from the beginning, which would surely reduce (if not destroy completely) the possibilities for a serious test of annihilation mechanisms.

Indeed, a good description of empirical  $\bar{N}N$  (elastic as well as charge-exchange) scattering data can be achieved with this model by adding a simple phenomenological, state- and energy-independent optical potential with only three parameters to account for annihilation [model A(BOX) [7]]. Thus, no arbitrary adjustment of the inner elastic part is *a priori* necessary in order to describe the empirical data. Obviously, this  $G$ -parity transform automatically provides the spin, isospin, and energy dependence which is phenomenologically required. This is an important finding in itself.

Turning things around, this elastic  $\bar{N}N$  interaction requires essentially no state, isospin, or energy dependence in the imaginary part and thus seems to support an absorptive disk picture as the dominant annihilation mechanism. However, this cannot be the end of the story. In order to come to reliable conclusions, it is essential to treat both the elastic and annihilation parts of the interaction consistently within the same microscopic framework.

It is clear that because of the complexity of the  $\bar{N}N$  annihilation channels this program becomes quite involved and can only be pursued in steps. In Ref. [7] we have started by evaluating a selected set of two-meson annihilation diagrams  $\bar{N}N \rightarrow M_1M_2 \rightarrow \bar{N}N$ , proceeding via baryon exchange. All combinations of those mesons whose exchanges are considered in the elastic  $\bar{N}N$  interaction (i.e.,  $\pi, \rho, \omega, \sigma, \delta$ ) have been included (with the same coupling constants) as well as the strange mesons  $K$  and  $K^*$  generated by hyperon exchange (with the corresponding coupling constants taken from our hyperon-nucleon model [8]).

However, since these channels account for at most about 30% of the total annihilation, their contributions have been artificially enhanced in Ref. [7] in order to provide the total empirical annihilation rate. (This has been achieved by suitably adjusting the form factor parameters.) This procedure of using only a few annihilation channels leads to a very pronounced state and isospin dependence of the annihilation interaction because of strict selection rules for each annihilation process as a consequence of the conservation of isospin, total angular momentum, parity, and  $G$  parity. This model (called C in Ref. [7]) therefore represents the other extreme as compared to the state-independent model A(BOX). As shown in Ref. [7], it actually fails to describe the empiri-

cal  $\bar{N}N \rightarrow \bar{N}N$  data quantitatively. Obviously, the state and isospin dependence of the corresponding annihilation interaction is too strong. (Certainly we could have improved the fit considerably by arbitrarily modifying inner part of both the elastic and annihilation interaction. Such a procedure, however, would completely obscure the message and, as we hope to have made clear, would be against the spirit of our approach.)

In a second step [9] we have predicted  $\bar{N}N \rightarrow M_1M_2$  transition rates proceeding via baryon exchange with adjustable form factor parameters. For this, a distorted-wave Born approximation (DWBA) procedure has been applied, with A(BOX) and C as the initial state interaction and no final (meson-meson) interaction. A reasonable agreement with the experimental situation could be achieved. However, there is a serious drawback of such a DWBA approach. The annihilation which occurs both in the initial state interaction and in the final transition process is treated inconsistently.

A consistent treatment can best be done in a coupled channels framework, which yields both  $\bar{N}N \rightarrow \bar{N}N$  and  $\bar{N}N \rightarrow M_1M_2$  amplitudes at the same time. Liu and Tabakin [10] demonstrated the need for such an approach in  $\bar{N}N$  physics and were the first to apply this method to explicit mesonic channels, namely,  $\pi\pi$  and  $\bar{K}K$ . With about 20 parameters (used to parametrize further effective channels and the short-range elastic part) they obtained a good simultaneous description of (elastic and charge-exchange)  $\bar{N}N$  scattering as well as  $\bar{N}N \rightarrow \pi\pi, \bar{K}K$  annihilation data.

In this paper, we present a consistent model describing  $\bar{N}N$  scattering and annihilation into specific channels at the same time, along the same lines. Compared to Ref. [10] the set of explicitly included meson channels is considerably enlarged. Namely, apart from the pseudoscalar mesons  $\pi, \eta, K$  we consider all possible combinations of the lowest-mass mesons with  $0^{++}, 1^{--}, 1^{++}, 2^{++}$  quantum numbers for both isospin  $I = 0$  and  $I = 1$ . This enlarged set of quantum numbers included and the fact that all two-meson channels are now employed with a realistic strength (in agreement with experimental information of annihilation) turns out to strongly reduce the state dependence of the annihilation interaction compared to our former model C and to decisively improve the description of the data, as will be demonstrated below.

As well as further two-meson channels with combinations of mesons not yet considered so far, there is a part remaining which could be made up from explicit three-meson channels or possible exotic contributions (glueballs, hybrids, etc.). In the model we present here, this part is taken into account by a phenomenological optical potential of similar form as used in model A(BOX) of Ref. [7], but, of course, with modified parameters since part of the annihilation is described microscopically.

The physical strength of the annihilation channels is determined by evaluating all  $\bar{N}N \rightarrow M_1M_2$  cross sections (at rest and in flight) and adjusting the form factor parameters at the annihilation vertices, which occur in both the initial state interaction and the final  $\bar{N}N \rightarrow M_1M_2$  transition, to available empirical information. This consistency in the choice of parameters is one major advan-

tage compared to the former calculation [9], in which model A(BOX) or C has been used as the initial state interaction.

In the next section, we describe our model for  $\bar{N}N$  scattering and annihilation. In Sec. III we present and discuss the results and compare these with our former models and experiment. Some concluding remarks are made in Sec. IV.

## II. MODEL FOR $\bar{N}N$ SCATTERING AND ANNIHILATION INTO TWO MESONS

In principle, the microscopic treatment of the  $\bar{N}N$  system is a complicated problem involving couplings between various baryonic and mesonic channels and diagonal interactions in all channels. In this paper we will suppress any diagonal interaction except in the  $\bar{N}N$  channel: The reason is that not much is known about these interactions, especially in the mesonic sector. Also, this approximation is not expected to severely affect the main purpose of this work, which is to demonstrate that an increased number of annihilation channels (with more meson quantum numbers  $J^{PC}$ ) treated explicitly reduces the state dependence of the microscopic annihilation model and so brings the result towards the experiment. The coupled equations for the  $\bar{N}N$  scattering amplitude  $T^{\bar{N}N \rightarrow \bar{N}N}$  and the transition amplitudes  $T^{\bar{N}N \rightarrow M_i M_j}$  for the annihilation into two mesons can then be written as

$$T^{\bar{N}N \rightarrow \bar{N}N} = V^{\bar{N}N \rightarrow \bar{N}N} + V^{\bar{N}N \rightarrow \bar{N}N} G^{\bar{N}N \rightarrow \bar{N}N} T^{\bar{N}N \rightarrow \bar{N}N}, \quad (1)$$

$$T^{\bar{N}N \rightarrow M_i M_j} = V^{\bar{N}N \rightarrow M_i M_j} + V^{\bar{N}N \rightarrow M_i M_j} G^{\bar{N}N \rightarrow \bar{N}N} T^{\bar{N}N \rightarrow \bar{N}N}. \quad (2)$$

The  $\bar{N}N$  interaction  $V^{\bar{N}N \rightarrow \bar{N}N}$  consists of an elastic and

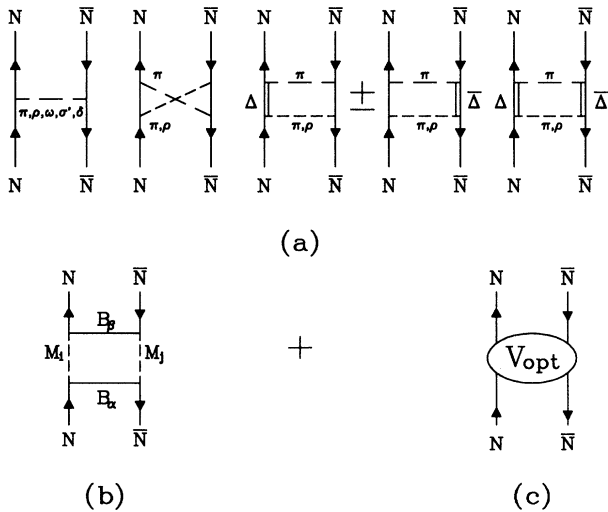


FIG. 1. Elastic (a), microscopic annihilation (b), and phenomenological annihilation (c) part of our  $\bar{N}N$  interaction model.

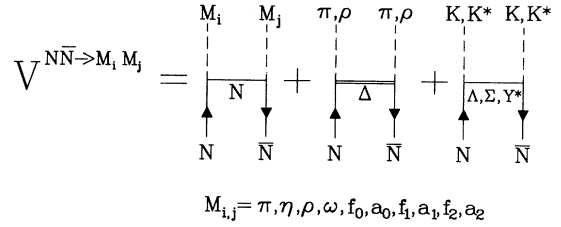


FIG. 2. Transition potentials  $V^{\bar{N}N \rightarrow M_i M_j}$  included explicitly in our microscopic annihilation model.

an annihilation part,

$$V^{\bar{N}N \rightarrow \bar{N}N} = V_{\text{el}} + V_{\text{ann}}. \quad (3)$$

As stated in the Introduction, we use the  $G$ -parity transform of the (slightly modified; cf. Ref. [7]) full Bonn  $NN$  potential [6] for that purpose. The corresponding diagrams are shown in Fig. 1(a). Compared to Ref. [7],  $V_{\text{ann}}$  is now split up into two parts,

$$V_{\text{ann}} = \sum_{ij} V^{M_i M_j \rightarrow \bar{N}N} G^{M_i M_j} V^{\bar{N}N \rightarrow M_i M_j} + V_{\text{opt}}. \quad (4)$$

The first part results from a microscopic treatment of various two-meson annihilation channels which proceed via baryon exchange [Fig. 1(b)]. It is important to realize that  $V^{\bar{N}N \rightarrow M_i M_j}$ , which occurs both in the  $\bar{N}N$  interaction [Eq. (4)] and in the actual annihilation process [Eq. (2)] is now treated with complete consistency.

The remaining contributions to the annihilation part

TABLE I. Coupling constants and cutoff parameters in the transition potential  $V^{\bar{N}N \rightarrow M_i M_j}$ .

Vertex	$\frac{g^2}{4\pi}$	$f/g$	$\Lambda$	$n$
$NN\pi$	0.0778		1500	1
$NN\eta$	0.6535		1500	1
$NN\rho$	0.84	6.1	1500	1
$NN\omega$	20.0	0	1500	1
$NNf_0$	5.723		1500	1
$NNa_0$	2.6653		1500	1
$NNf_1$	10.0		1500	1
$NNa_1$	7.0		1500	1
$NNf_2$	2.0		1500	2
$NNa_2$	4.0		1500	2
$N\Delta\pi$	0.224		1700	1
$N\Delta\rho$	20.45		1700	2
$N\Delta K$	0.9063		1800	1
$N\Delta K^*$	2.5217	-5.175	1800	1
$N\Sigma K$	0.0313		2000	1
$N\Sigma K^*$	0.8409	2.219	2000	1
$NY^* K$	0.0372		2000	1
$NY^* K^*$	3.4077		2000	2

of the  $\bar{N}N$  interaction (involving, e.g., the explicit transition into three and more mesons) will now be taken into account by an additional phenomenological piece [Fig. 1(c)], for which we use the following parametrization in coordinate space:

$$V_{\text{opt}} = iW e^{-\frac{r^2}{2r_0^2}}. \quad (5)$$

It is completely independent of energy, spin, and isospin, with two parameters ( $W = -1$  GeV,  $r_0 = 0.4$  fm) adjusted to the  $\bar{N}N \rightarrow \bar{N}N$  cross section data.

TABLE II. Conservation of parity and  $G$  parity impose selection rules on the transition from the  $\bar{N}N$  system to the two-meson system: All hatched fields are generally forbidden by parity conservation. Transitions marked by the letter A are allowed for meson pair parity  $G' = (-1)^{(I+J)}$ , whereas transitions marked by B can occur for  $G' = (-1)^{(I+J+1)}$ .

	Meson state		$\bar{N}N$ state		
			$L = J$ $S = 0$	$L = J$ $S = 1$	$L = J \pm 1$ $S = 1$
<i>PP</i>	$L' = J$	$S' = 0$			A
<i>PS</i>	$L' = J$	$S' = 0$	A	B	
<i>SS</i>	$L' = J$	$S' = 0$			A
<i>VP</i>	$L' = J$	$S' = 1$			A
	$L' = J \pm 1$	$S' = 1$	A	B	
<i>VS</i>	$L' = J$	$S' = 1$	A	B	
	$L' = J \pm 1$	$S' = 1$			A
<i>AP</i>	$L' = J$	$S' = 1$	A	B	
	$L' = J \pm 1$	$S' = 1$			A
<i>VV</i>	$L' = J$	$S' = 0$			A
	$L' = J$	$S' = 1$			A
	$L' = J \pm 1$	$S' = 1$	A	B	
	$L' = J$	$S' = 2$			A
	$L' = J \pm 1$	$S' = 2$	A	B	
	$L' = J \pm 2$	$S' = 2$			A
<i>AV</i>	$L' = J$	$S' = 0$	A	B	
	$L' = J$	$S' = 1$	A	B	
	$L' = J \pm 1$	$S' = 1$			A
	$L' = J$	$S' = 2$	A	B	
	$L' = J \pm 1$	$S' = 2$			A
	$L' = J \pm 2$	$S' = 2$	A	B	
<i>TP</i>	$L' = J$	$S' = 2$	A	B	
	$L' = J \pm 1$	$S' = 2$			A
	$L' = J \pm 2$	$S' = 2$	A	B	
<i>TV</i>	$L' = J$	$S' = 1$	A	B	
	$L' = J \pm 1$	$S' = 1$			A
	$L' = J$	$S' = 2$	A	B	
	$L' = J \pm 1$	$S' = 2$			A
	$L' = J \pm 2$	$S' = 2$	A	B	
	$L' = J$	$S' = 3$	A	B	
	$L' = J \pm 1$	$S' = 3$			A
	$L' = J \pm 2$	$S' = 3$	A	B	
	$L' = J \pm 3$	$S' = 3$			A

In our model, the sum over  $i, j$  in Eq. (4) goes over all possible combinations of  $\pi, \eta, \rho, \omega, a_0, f_0, a_1, f_1, a_2, f_2$  (via  $N, \Delta$  exchange) and  $K, K^*$  (via  $\Lambda, \Sigma, Y^*$  exchange); cf. Fig. 2. In order to obtain the transition interactions  $V^{\bar{N}N \rightarrow M_1 M_2}$  we start from interaction Lagrangians given in the Appendix. As in the Bonn potential, the corresponding diagrams have been evaluated within time-ordered perturbation theory. Explicit expressions and details can be found in [7,9].

So far as parameters are concerned, many of the coupling constants are already used in the Bonn potential [6] and the Juelich hyperon-nucleon model [8]. They are identical to those used in the elastic interaction. The remaining coupling constants are chosen in line with empirical information [11]. Only those without any information had to be fitted to the  $\bar{N}N$  cross sections. Furthermore, the vertex functions contain form factors, parametrized in a monopole-type form

$$F(\vec{p}_\delta^2) = \left( \frac{\Lambda_\delta^2 - M_\delta^2}{\Lambda_\delta^2 + \vec{p}_\delta^2} \right)^n, \quad (6)$$

where  $\vec{p}_\delta$  ( $M_\delta$ ) is the three-momentum (mass) of the baryon exchanged in  $V^{\bar{N}N \rightarrow M_1 M_2}$ .

Note that these form factors used in the annihilation diagrams have to be distinguished from those used in the elastic meson-exchange process (although the same particles are involved at the vertex) since now the exchanged baryon is the essential off-shell particle. Therefore the form factor is needed in a quite different kinematic region. The parameter  $\Lambda_\delta$  should depend on the type of particles involved at the vertex. However, in order to reduce the number of free parameters, we allow  $\Lambda$  to depend only on the type of the exchanged baryon but not on the produced meson. The values actually used are given in Table I; they have been fixed in a self-consistency procedure to reproduce empirical annihilation data; see Sec. III.

We mention finally that the conservation of parity  $P$  and parity  $G$  (respectively, charge conjugation  $C$ ) results in the following conditions (here the primed magnitudes refer to the two-meson system, the unprimed ones to the  $\bar{N}N$  system):

$$(-1)^{L+S+I} = \begin{cases} G_i G_j & \text{if } M_i, M_j \\ & \text{are } G \text{ eigenstates,} \\ (-1)^{L'+S'+I} & \text{otherwise,} \end{cases} \quad (7)$$

$$(-1)^{L+1} = P_i P_j (-1)^{L'}. \quad (7)$$

The resulting selection rules are presented graphically in Table II.

### III. RESULTS AND DISCUSSION

The model specified in the last section (called model D in the following) provides definite predictions for both the  $\bar{N}N$  scattering and annihilation amplitude [Eqs. (1),(2)]. From these, cross sections and spin observables can be obtained in a straightforward way. Throughout we will compare the results of model D with corresponding results of the preceding models A (BOX) and C [7].

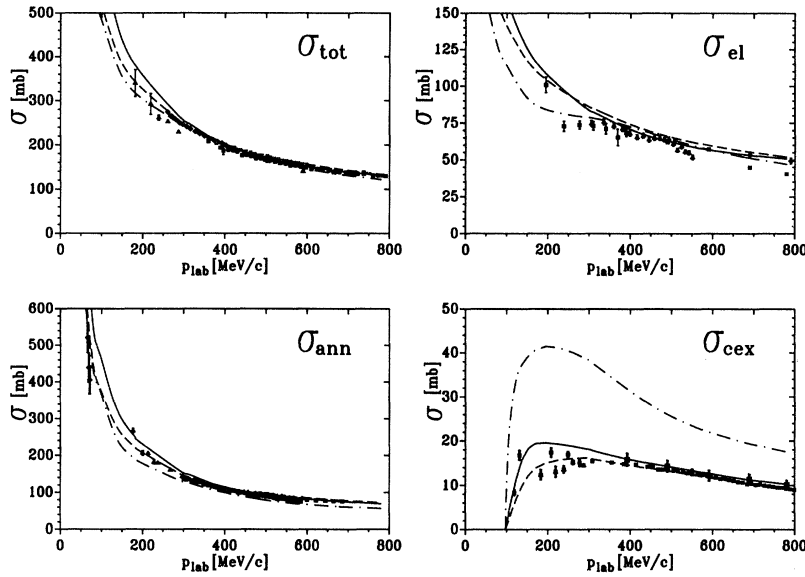


FIG. 3. Total, elastic, charge-exchange, and annihilation cross sections for  $\bar{p}p$  scattering. Results of the consistent model D are given by the solid lines, dashed lines correspond to the phenomenological model A(BOX), and dashed-dotted lines result from the effective microscopic model C. The references for the data can be found in Refs. [2,16].

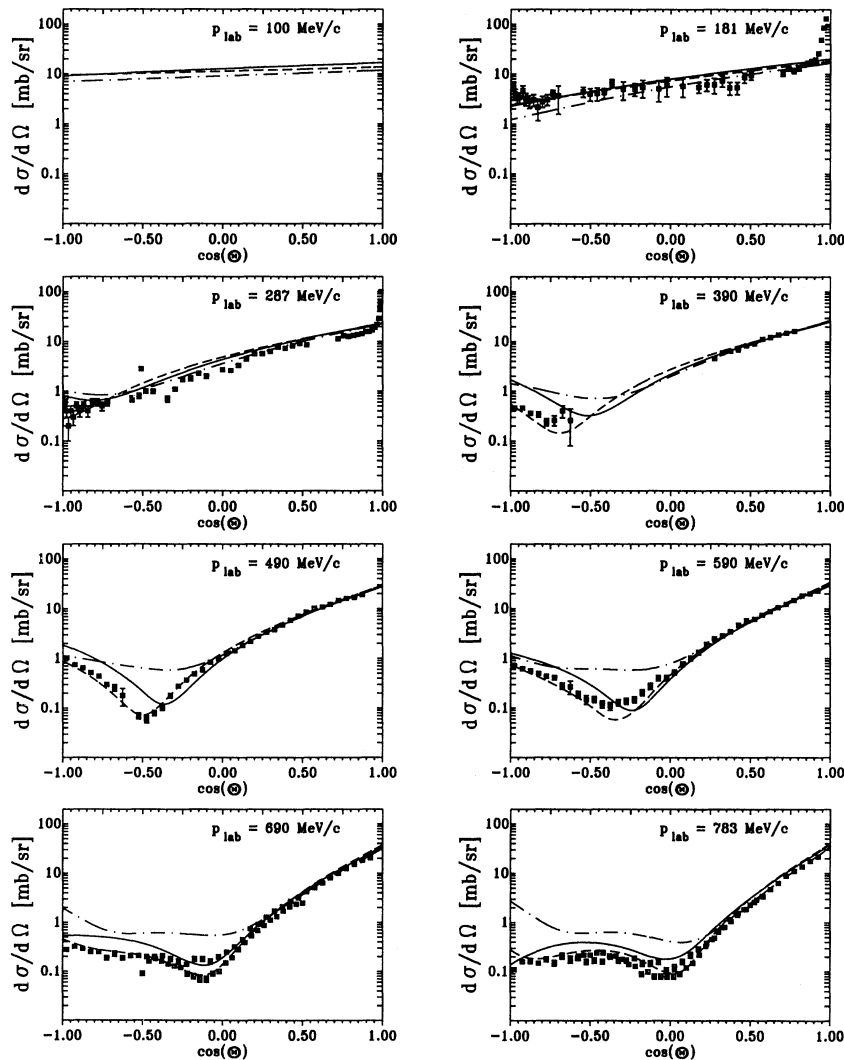


FIG. 4. Elastic  $\bar{p}p$  differential cross sections at various energies. The data are taken from Refs. [17–21]. The same description of the curves as in Fig. 3.

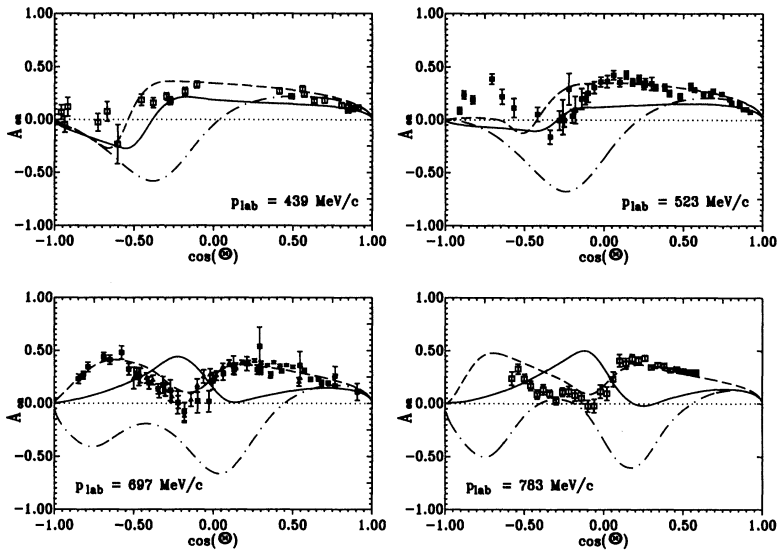


FIG. 5. Elastic  $\bar{p}p$  polarizations at some energies. The data are taken from Refs. [17-21]. The same description of the curves as in Fig. 3.

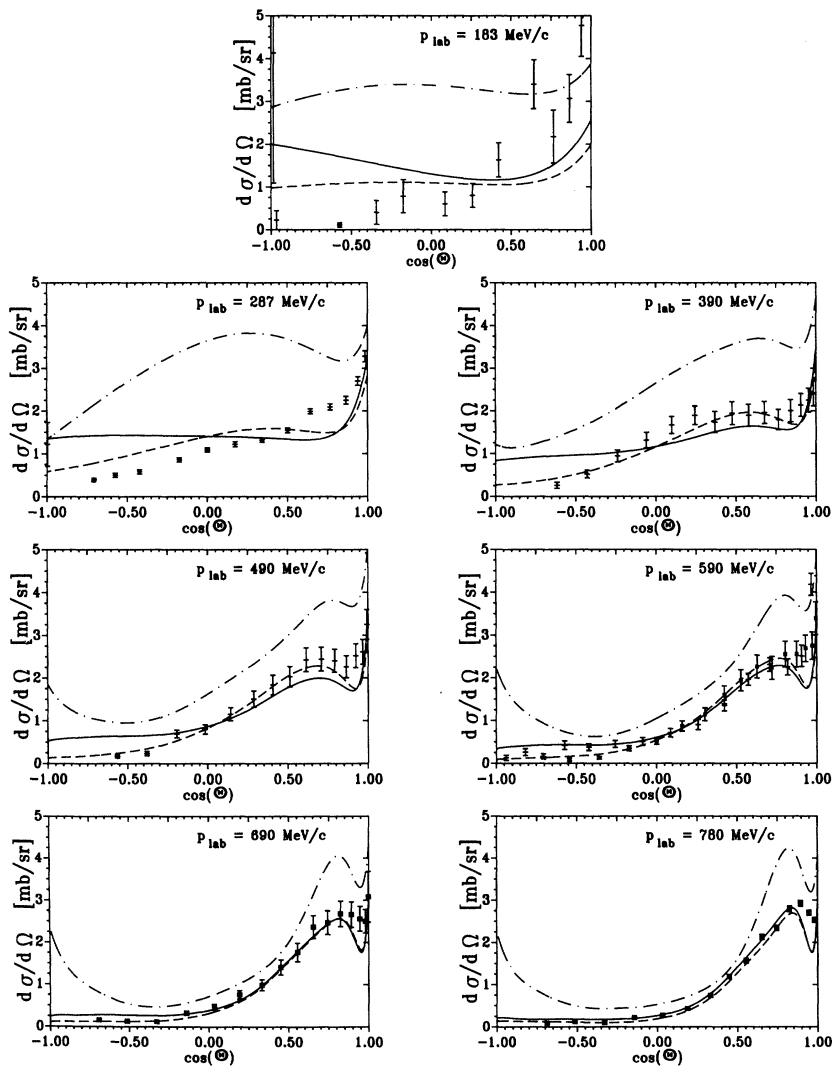


FIG. 6. Charge-exchange differential cross sections. The data are taken from Refs. [22-24]. The same description of the curves as in Fig. 3.

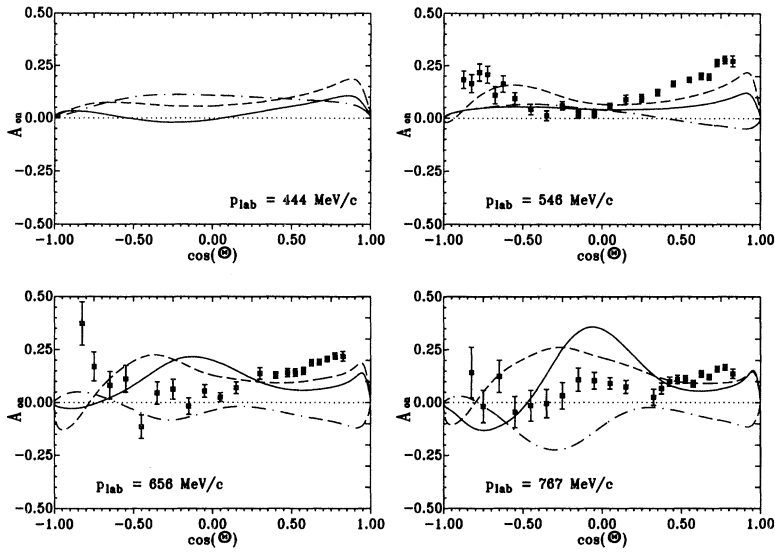


FIG. 7. Charge-exchange polarizations. The data are taken from Refs. [22–24]. The same description of the curves as in Fig. 3.

### A. $\bar{N}N$ scattering

Figure 3 shows the total, integrated elastic, and charge exchange as well as the annihilation cross sections for  $\bar{p}p$  scattering. Models D and A(BOX) of Ref. [7] (which contains absolutely no isospin dependence for the annihilation part) agree with the empirical data. In contrast,

the result of the effective microscopic model C of Ref. [7] is by about a factor of 2 too large in the charge-exchange cross section. This is because the isospin dependence of this annihilation model is too strong, being generated by only a few annihilation channels.

Results for the differential cross sections for elastic ( $\bar{p}p \rightarrow \bar{p}p$ ) scattering are shown in Fig. 4. The differential cross section is essentially flat for low energies, while al-

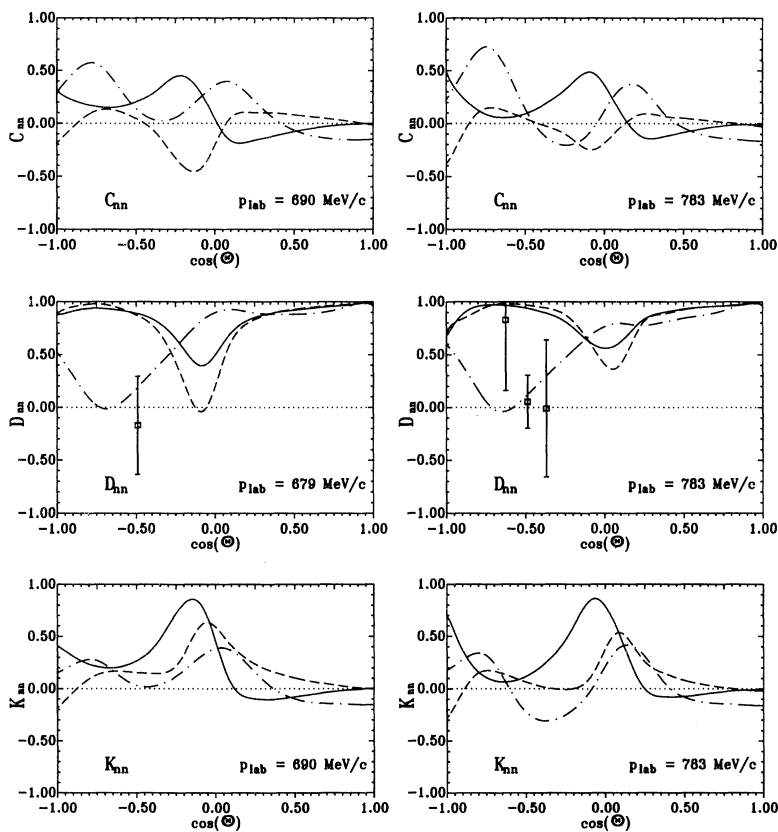


FIG. 8. Some spin observables in the elastic channel:  $C_{nn}$ ,  $D_{nn}$ , and  $K_{nn}$  at two different energies. The data are taken from Ref. [12]. The same description of the curves as in Fig. 3.

ready for moderate energies a strong forward peak is seen, which clearly demonstrates the importance of higher partial waves. For the highest energy considered here, a minimum is observed in the cross section because diffractive effects become relevant. Throughout, model A(BOX) provides a good description; the agreement with the data is still reasonable for the consistent annihilation model D but fails completely for the effective model C. A similar situation is found for the elastic polarization (Fig. 5). Model D accounts for the basic structures at low energies although there are deficiencies at higher energies. A rather reasonable agreement can be achieved with model A(BOX), while model C predicts the wrong sign.

The results of model D and model A(BOX) for the differential cross section of the charge-exchange reaction  $\bar{p}p \rightarrow \bar{n}n$  (Fig. 6) almost coincide at higher energies. For low energies, however, differences occur at backward angles. It has already been noted in the discussion of the integrated cross section that the effective annihilation model C cannot provide a description of this process due to a too strong isospin sensitivity of the annihilation.

The description of the charge-exchange polarization data (Fig. 7) is still unsatisfactory, especially at backward angles and higher energies.

At the end of this section we show also the results for some selected spin observables at two different energies, for both the elastic (Fig. 8) and the charge-exchange channels (Fig. 9). For the elastic spin-transfer observable

$D_{nn}$  a few data points have been measured [12], data have been obtained recently for the charge-exchange  $D_{nn}$  [13].

In summary, the increased number of explicit mesonic channels included consistently, with a realistic strength, has obviously improved the state dependence of our baryon-exchange annihilation model considerably. On the other hand, the comparison with the phenomenological annihilation model A(BOX) shows that important physics is still missing. Again, we certainly had the possibility to improve the agreement between the model D results and experimental data, e.g., by adding spin-dependent (spin-orbit, tensor) parts to the optical potential [Eq. (5)]. For the reasons already discussed in the Introduction we resisted this temptation.

## B. Annihilation into two mesons

In the following section we will look at the results for specific annihilation channels.

Most data for the annihilation into two mesons are obtained from the annihilation at rest in liquid or gaseous hydrogen [1,2]. Table III contains all the relative cross sections for the 53 annihilation channels included in our consistent annihilation model D. In order to demonstrate the influence of the initial state interaction we

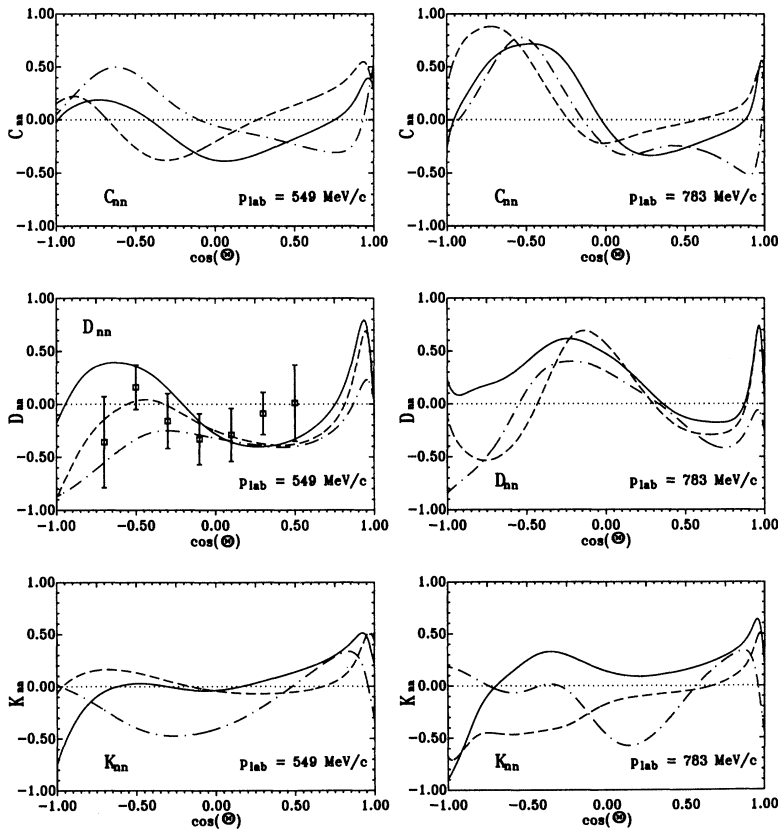


FIG. 9. The spin observables  $C_{nn}$ ,  $D_{nn}$ , and  $K_{nn}$  for the charge-exchange reaction. The data are taken from Ref. [13]. The same description of the curves as in Fig. 3.



also show the results (with unchanged transition potential parameters) when A(BOX) is used instead of D as the initial state interaction. The largest contributions are given by the combinations of two vector mesons. Vector-

TABLE III. Branching ratios "at rest" for 53 annihilation channels. The data are taken from Refs. [1,2].

$\bar{p}p \rightarrow$	D	A(BOX)	Expt.
$\pi^+\pi^-$	0.54	0.92	$0.33 \pm 0.017$
$\pi^0\pi^0$	0.098	0.33	$0.02 - 0.06$
$\pi^0\eta$	0.0095	0.01	$0.03 \pm 0.02$
$\eta\eta$	0.0037	0.0075	$0.008 \pm 0.003$
$\pi^\pm a_0^\mp$	0.013	0.017	$0.69 \pm 0.12$
$\pi^0 a_0^0$	0.0021	0.0046	
$\eta a_0^0$	0.021	0.014	
$\pi^0 f_0$	0.067	0.035	
$\eta f_0$	0.0090	0.024	
$a_0^+ a_0^-$	0.0017	0.0011	
$a_0^0 a_0^0$	0.0007	0.0005	
$f_0 a_0^0$	0.0002	0.0002	
$f_0 f_0$	0.0008	0.0006	
$\rho^\pm \pi^\mp$	2.32	3.94	$3.4 \pm 0.2$
$\rho^0 \pi^0$	0.85	1.21	$1.4 \pm 0.1$
$\rho^0 \eta$	0.09	0.64	$0.65 \pm 0.14$
$\omega \pi^0$	0.57	2.11	$0.52 \pm 0.05$
$\omega \eta$	0.20	0.09	$0.46 \pm 0.14$
$\rho^\pm a_0^\mp$	0.63	0.40	
$\rho^0 a_0^0$	0.24	0.13	
$\rho^0 f_0$	0.90	1.82	
$\omega a_0^0$	0.17	0.70	
$\omega f_0$	1.28	1.90	
$a_1^\pm \pi^\mp$	1.03	0.83	
$a_1^0 \pi^0$	0.22	0.17	
$a_1^0 \eta$	0.0078	0.0088	
$f_1 \pi^0$	0.47	0.63	
$f_1 \eta$	0.0033	0.0032	
$\rho^+ \rho^-$	4.30	16.8	$(< 9.5)$
$\rho^0 \rho^0$	1.04	2.20	$0.4 \pm 0.3$
$\rho^0 \omega$	2.13	3.94	$3.9 \pm 0.6$
$\omega \omega$	1.07	1.62	$1.4 \pm 0.6$
$\rho^\pm a_1^\mp$	0.099	0.99	
$\rho^0 a_1^0$	0.028	0.14	
$\omega a_1^0$	3.76	2.26	
$\rho^0 f_1$	0.039	0.029	
$a_2^\pm \pi^\mp$	0.88	0.74	$1.3-2.6$
$a_2^0 \pi^0$	0.14	0.18	
$f_2 \eta$	0.0026	0.0032	
$a_2^0 \eta$	0.0025	0.0026	
$f_2 \pi^0$	0.068	0.078	$0.41 \pm 0.12$
$a_2^\pm \rho^\mp$	0.040	0.028	
$a_2^0 \rho^0$	0.013	0.0052	
$f_2 \rho^0$	0.067	0.071	$1.57 \pm 0.34$
$f_2 \omega$	0.14	0.10	$3.05 \pm 0.31$
$K^+ K^-$	0.065	0.095	$0.1 \pm 0.01$
$K^0 \bar{K}^0$	0.0041	0.024	$0.08 \pm 0.01$
$K^\pm K^{*\mp}$	0.050	0.46	$0.1 \pm 0.016$
$K^0 \bar{K}^{*0}$			
$/K^{*0} K^0$	0.0044	0.025	$0.12 \pm 0.02$
$K^{*+} K^{*-}$	0.055	0.19	$0.13 \pm 0.05$
$K^{*0} \bar{K}^{*0}$	0.023	0.035	$0.26 \pm 0.05$
$\Sigma$	23.77	45.96	$30.94 \pm 3.91$

pseudoscalar and vector-axial-vector combinations also provide sizable fractions of the total annihilation. These findings are independent of the particular initial state interaction model used and are determined by the relevant vertex structures in the baryon-exchange diagrams. Other channels or combinations are of minor importance; however, they tend to weaken the state dependence of the total annihilation, a feature obviously favored by the empirical data. Some channels can be reached for an annihilation at rest only when the width of the mesons is taken into account, because the sum of their rest masses is larger than twice the nucleon mass.

The fit of these branching ratios can certainly be improved by relaxing the condition that the cutoff mass  $\Lambda$  in the baryon-exchange diagrams does not depend on the meson produced. For example, for nucleon exchange, the value  $\Lambda_N = 1.5$  GeV is mainly determined from the experimentally well known annihilation channels involving  $\pi$ ,  $\rho$ , and  $\omega$ . For spin-2 mesons ( $a_2, f_2$ ) the required dipole form ( $n = 2$ ) then leads to a relative suppression, which could be counterbalanced by a higher value of  $\Lambda$ . As seen from Table III, this would bring the theoretical results in better agreement with experiment.

A great success of the recent experiments done at LEAR is the measurement of branching ratios together with the determination of the quantum numbers of the initial  $\bar{N}N$  state [2]. Table IV shows ratios for either the same initial  $\bar{N}N$  state into different annihilation channels or into the same channel from different initial  $\bar{N}N$  states. These ratios express so-called dynamical selection rules; a famous example is the first one (" $\pi\rho$  puzzle"). Those annihilation channels which are in principle allowed by the fundamental quantum number conservation do not

TABLE IV. Ratios of branching ratios "at rest" for some interesting channels as examples for dynamical selection rules. The data are taken from Refs. [1,2].

	D	A(BOX)	Born	Expt.
$\frac{\bar{p}p (^3S_1, I=0) \rightarrow \rho^\pm \pi^\mp}{\bar{p}p (^1S_0, I=1) \rightarrow \rho^\pm \pi^\mp}$	4.67	2.29	3.45	$35 \pm 16$
$\frac{\bar{p}p (^1P_1, I=0) \rightarrow \rho^\pm \pi^\mp}{\bar{p}p (^3P_{1,2}, I=1) \rightarrow \rho^\pm \pi^\mp}$	0.34	0.11	0.19	$1.16 \pm 0.23$
$\frac{\bar{p}p (^1S_0, I=1) \rightarrow f_2 \pi^0}{\bar{p}p (^1S_0, I=1) \rightarrow \rho^\pm \pi^\mp}$	0.28	0.11	0.056	2.6
$\frac{\bar{p}p (^3P_1, I=1) \rightarrow f_2 \pi^0}{\bar{p}p (^3P_2, I=1) \rightarrow f_2 \pi^0}$	1.49	1.57	1.23	$\approx 11$
$\frac{\bar{p}p (^1S_0, I=0) \rightarrow a_2^\pm \pi^\mp}{\bar{p}p (^3S_1, I=1) \rightarrow a_2^\pm \pi^\mp}$	0.51	0.93	0.91	$3.6-8$
$\frac{\bar{p}p (^1S_0, I=0) \rightarrow \rho^0 \rho^0}{\bar{p}p (^1S_0, I=0) \rightarrow \omega \omega}$	6.30	62.40	1.76	$0.1-0.3$
$\frac{\bar{p}p (^1S_0, I=1) \rightarrow \rho^0 \omega}{\bar{p}p (^1S_0, I=0) \rightarrow \omega \omega}$	13.17	4.23	4.33	0.8
$\frac{\bar{p}p (^3S_1, I=1) \rightarrow \rho^0 \eta}{\bar{p}p (^3S_1, I=0) \rightarrow \omega \eta}$	0.47	10.95	0.98	$0.55 \pm 0.12$

occur with equal probability or a statistical distribution; the rate obviously depends sensitively on the channels and the involved dynamics. Ratios like those shown in Table IV are often supposed to minimize the effects of the initial (and final) state interactions. However, as clearly seen from the table, there is a strong sensitivity to whether and even which kind of initial state interaction is included. It does not drop out even if ratios from the same partial wave are considered. (Note that the numbers of Table III increase by an order of magnitude if calculated in Born approximation.) Thus a consistent description for the transition model, initial state interaction (and probably also final state interaction) is required before one can seriously address the question about which transition mechanism is preferred. Conclusions based on the Born approximation appear to be premature.

For the most important annihilation channels cross section data for the annihilation in flight exist (see Fig. 10), which illustrate the energy dependence of the annihilation mechanism. Obviously, model D leads to a satisfactory overall description.

For the  $\pi^+\pi^-$  and the  $\bar{K}K$  channels some more sensitive observables have been measured, too: the differential cross section and the analyzing power [14]. It has been shown in Ref. [15] that the description of both these observables requires more effort: Here the interactions between the outgoing mesons (which are to some extent known in this case) seem to be essential for the reproduction of the experimentally observed features of the data. Work is in progress to do a coupled channels calculation for these annihilation channels including also  $\pi\pi \rightarrow \pi\pi$ ,  $\pi\pi \rightarrow \bar{K}K$ , and  $\bar{K}K \rightarrow \bar{K}K$  interactions and in this way try to describe also these high-quality angle-dependent data.

#### IV. CONCLUDING REMARKS

One of the main topics of current research is to identify the relevant degrees of freedom in low- and medium-energy strong interaction physics. The short-range part

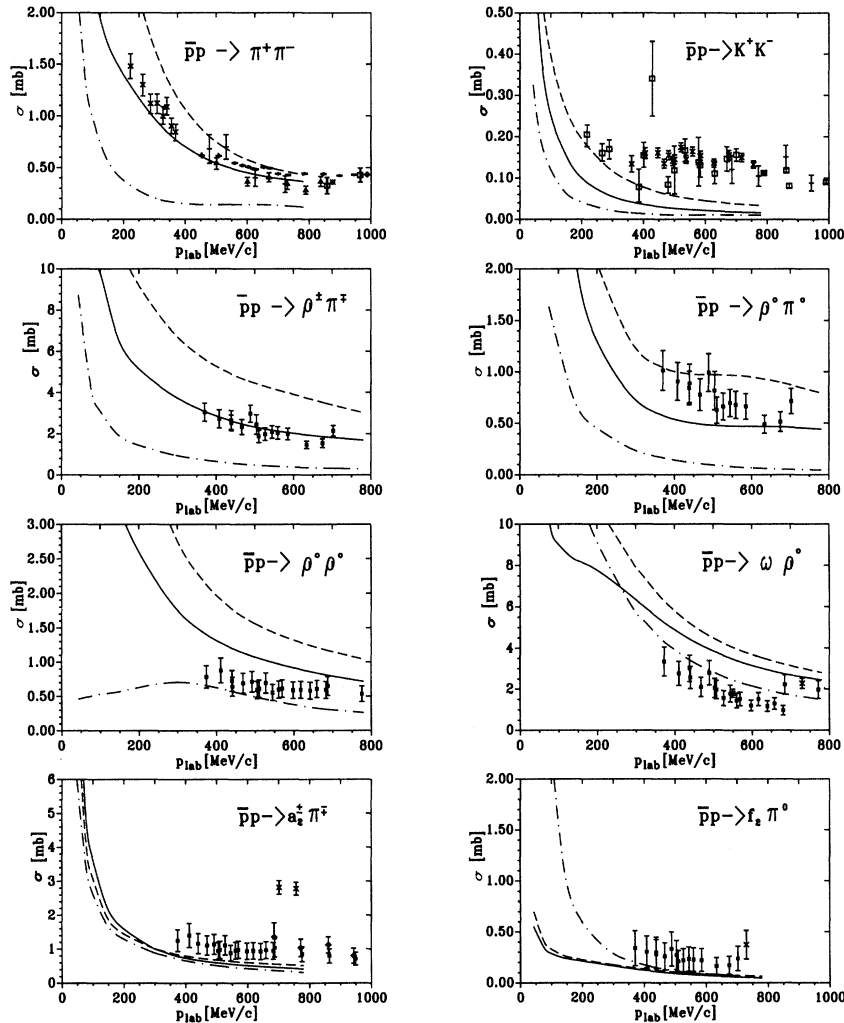


FIG. 10. Annihilation cross sections “in flight” for the most important channels. The same description of the curves as in Fig. 3. The data are calculated from values given in Refs. [25,26].

of the  $\bar{N}N$  interaction represents a particular challenge in this respect, as a result of the considerable complexities introduced by the coupling of various mesonic channels. In order to come to reliable conclusions, a consistent description of not only  $\bar{N}N$  scattering but also annihilation phenomena in specific mesonic channels is required, with full inclusion of initial and final state interaction effects. Such a program can be best done in a coupled channels framework. Since it requires an enormous effort it can only be done in steps by increasing the number of explicit channels and/or including more and more diagonal mesonic interactions. In this procedure it is advisable to keep the number of free parameters small in order to avoid fitting the data quantitatively while still missing a lot of important physics in the model.

In this paper, we have presented a conventional hadronic model, in terms of meson and baryon exchange, which enables a simultaneous prediction of  $\bar{N}N$  scattering and annihilation phenomena in the two-meson sector involving the lowest-mass  $J^P = 0^\pm, 1^\pm, 2^+$  mesons for both isospin  $I = 0$  and  $I = 1$ . Given that we have only about ten energy-independent free parameters (some open coupling constants, five cutoff masses in the baryon-exchange diagrams, and two optical potential parameters), the results presented are, in our opinion, already quite encouraging proving at least that also in the  $\bar{N}N$  sector the conventional hadronic concept is worth pursuing further and is surely a valid alternative to quark-gluon models. Still, remaining discrepancies to empirical data (especially in the spin observables) are a reflection of the fact that important physics is still missing. Apart from further mesonic channels, diagonal mesonic interactions as well as direct couplings between the various mesonic channels have to be included, which represents a challenging task for the future.

## APPENDIX: INTERACTION LAGRANGIANS

The following Lagrangians are used in this work for the coupling of spin- $\frac{1}{2}$  baryons and mesons:

$$\mathcal{L}_{BBS} = g_{BBS} \bar{\Psi}_\alpha \Psi_\beta \Phi^j, \quad (\text{A1})$$

$$\mathcal{L}_{BBP} = \frac{g_{BBP}}{m_p} \bar{\Psi}_\alpha \gamma^5 \gamma^\mu \Psi_\beta \partial_\mu \Phi^j, \quad (\text{A2})$$

$$\mathcal{L}_{BBV} = g_{BBV} \bar{\Psi}_\alpha \gamma^\mu \Psi_\beta \Phi_\mu^j + \frac{f_{BBV}}{4M_N} \bar{\Psi}_\alpha \sigma^{\mu\nu} \Psi_\beta (\partial_\mu \Phi_\nu^j - \partial_\nu \Phi_\mu^j), \quad (\text{A3})$$

$$\mathcal{L}_{BBA} = g_{BBA} \bar{\Psi}_\alpha \gamma^5 \gamma^\mu \Psi_\beta \Phi_\mu^j, \quad (\text{A4})$$

$$\mathcal{L}_{BBT} = \frac{g_{BBT}}{M_N} \{i\bar{\Psi}_\alpha (\gamma^\mu \partial^\nu \Psi_\beta + \gamma^\nu \partial^\mu \Psi_\beta) - i(\partial^\nu \bar{\Psi}_\alpha \gamma^\mu + \partial^\mu \bar{\Psi}_\alpha \gamma^\nu) \Psi_\beta\} \Phi_{\mu\nu}^j. \quad (\text{A5})$$

Vertices with a spin- $\frac{1}{2}$  and a spin- $\frac{3}{2}$  baryon and a meson are given by the Lagrangians

$$\mathcal{L}_{BDP} = \frac{g_{BDP}}{m_p} \bar{\Psi}_\alpha \Psi_\beta^\mu \partial_\mu \Phi^j, \quad (\text{A6})$$

$$\mathcal{L}_{BDV} = \frac{g_{BDV}}{m_v} \bar{\Psi}_\alpha i\gamma^5 \gamma^\mu \Psi_\beta^\nu (\partial_\mu \Phi_\nu^j - \partial_\nu \Phi_\mu^j), \quad (\text{A7})$$

with the following meaning of the indices:  $B$  spin- $\frac{1}{2}$  baryons;  $D$  spin- $\frac{3}{2}$  baryons;  $S$  scalar mesons,  $J^P = 0^+$ ;  $P$  pseudoscalar mesons,  $J^P = 0^-$ ;  $V$  vector mesons,  $J^P = 1^-$ ;  $A$  axial-vector mesons,  $J^P = 1^+$ ;  $T$  tensor mesons,  $J^P = 2^+$ .

- 
- [1] C. Amsler and F. Myhrer, *Annu. Rev. Nucl. Part. Sci.* **41**, 219 (1991).
  - [2] C.B. Dover, T. Gutsche, M. Maruyama, and A. Fässler, *Prog. Part. Nucl. Phys.* **29**, 87 (1992).
  - [3] P.H. Timmers, W.A. van der Sanden, and J.J. de Swart, *Phys. Rev. D* **29**, 1928 (1984); R. Timmermans, Th.A. Rijken, and J.J. de Swart, *Phys. Rev. C* **50**, 48 (1994).
  - [4] M. Pignone, M. Lacombe, B. Loiseau, and R. Vinh Mau, *Phys. Rev. C* **50**, 2710 (1994).
  - [5] G. Janssen, K. Holinde, and J. Speth, *Phys. Rev. Lett.* **73**, 1332 (1994).
  - [6] R. Machleidt, K. Holinde, and Ch. Elster, *Phys. Rep.* **149**, 1 (1987).
  - [7] T. Hippchen, J. Haidenbauer, K. Holinde, and V. Mull, *Phys. Rev. C* **44**, 1323 (1991).
  - [8] B. Holzenkamp, K. Holinde, and J. Speth, *Nucl. Phys.* **A500**, 485 (1989).
  - [9] V. Mull, J. Haidenbauer, T. Hippchen, and K. Holinde, *Phys. Rev. C* **44**, 1337 (1991).
  - [10] G.Q. Liu and F. Tabakin, *Phys. Rev. C* **41**, 665 (1990).
  - [11] O. Dumbrais *et al.*, *Nucl. Phys.* **B216**, 277 (1983).
  - [12] R.A. Kunne *et al.*, *Phys. Lett. B* **261**, 191 (1991).
  - [13] A. Ahmidouch, Ph.D. thesis, University of Genève, 1994.
  - [14] A. Hasan *et al.*, *Nucl. Phys.* **B378**, 3 (1992).
  - [15] V. Mull, K. Holinde, and J. Speth, *Phys. Lett. B* **275**, 12 (1992).
  - [16] V. Mull, Ph.D. thesis, Universität Bonn, 1993; Berichte des Forschungszentrums Jülich No. 2844, 1993.
  - [17] W. Brückner *et al.*, *Phys. Lett.* **166B**, 113 (1986).
  - [18] M. Kimura *et al.*, *Nuovo Cimento A* **71**, 438 (1982).
  - [19] R.A. Kunne *et al.*, *Phys. Lett. B* **206**, 557 (1988); R.A. Kunne *et al.*, *Nucl. Phys.* **B323**, 1 (1989).
  - [20] R. Bertini *et al.*, *Phys. Lett. B* **228**, 531 (1989); F. Perrot-Kunne *et al.*, in *Proceedings of the 1st Biennial Conference on Low Energy Antiproton Physics*, Stockholm, 1990, edited by P. Carlson, A. Kerek, and S. Szilagy (World Scientific, Singapore, 1991), p. 251.
  - [21] T. Kageyama, T. Fujii, K. Nakamura, F. Sai, S. Sakamoto, S. Sato, T. Takahashi, T. Tanimori, and S.S. Yamamoto, *Phys. Rev. D* **35**, 2655 (1987).
  - [22] K. Nakamura, T. Fujii, T. Kageyama, F. Sai, S. Sakamoto, S. Sato, T. Takahashi, T. Tanimori, S.S. Yamamoto, and Y. Takada, *Phys. Rev. Lett.* **53**, 885 (1984).

- [23] W. Brückner *et al.*, Phys. Lett. **169B**, 302 (1986).
- [24] R. Birsa *et al.*, Phys. Lett. B **246**, 267 (1990).
- [25] G. Bardin *et al.*, in *Proceedings of the 1st Biennial Conference on Low Energy Antiproton Physics*, Stockholm, 1990, edited by P. Carlson, A. Kerek, and S. Szilagyi (World Scientific, Singapore, 1991), p. 173.
- [26] F. Sai, S. Sakamoto, and S.S. Yamamoto, Nucl. Phys. **B213**, 371 (1983).